A RSM METHOD FOR NONLINEAR PROBABILISTIC ANALYSIS OF THE REINFORCED CONCRETE STRUCTURE FAILURE OF A NUCLEAR POWER PLANT – TYPE VVER 440

Juraj Králik*

This paper describes the reliability analysis of a concrete containment for VVER 440 under a high internal overpressure. The probabilistic safety assessment (PSA) level 3 aims at an assessment of the probability of the concrete structure failure under the excessive overpressure. The non-linear analysis of the concrete structures was considered. The uncertainties of the loads level (long-time temperature and dead loads), the material model (concrete cracking and crushing, behavior of the reinforcement and liner), degradation effects and other influences following from the inaccuracy of the calculated model and numerical methods were taken into account in the response surface method (RSM). The results of the reliability analysis of the NPP structures are presented.

Keywords: *nuclear power plant VVER, probabilistic safety analysis, concrete failure, RSM, ANSYS*

1. Introduction

The International Atomic Energy Agency set up a program to give guidance to its member states on many aspects of the safety of nuclear power reactors. In the case of the analysis PSA 3 level it is necessary to determine the probability of the concrete structure failure under higher overpressure. The general purpose of the probabilistic analysis of the containment integrity failure was to define the critical places of the structure elements and to estimate the structural collapse. In this paper the nonlinear analysis of the concrete containment resistance for mean values of loads, material properties and the overpressure higher than Beyond Design Basic Accident (BDBA) are presented. Following these results the probability check of the structural integrity can be performed for the random value of the loads and material characteristics by the RSM method [4, 15, 16 and 17].

The object of NPP V1 is rectangular in the plan (Figure 1). There are two critical structures – the containment (CTMT) and the emergency water safety tank (EWST). The foundation conditions under the NPP V1 structure are also complicated.

The complicated wall configuration inside the hermetic zone provides more possibilities for the occurrence of local peak stress along the contact of walls and plates. The computational FEM model of the NPP V1 structures is presented in Figure 2.

For a complex analysis of the reinforced concrete structure of the hermetic zone for different kinds of loads, the ANSYS software and the CRACK program [12 and 13] (created by

* prof. Ing. J. Králik, PhD., Slovak University of Technology, Faculty of Civil Engineering, Department of Structural Mechanics, Radlinského 11, Bratislava

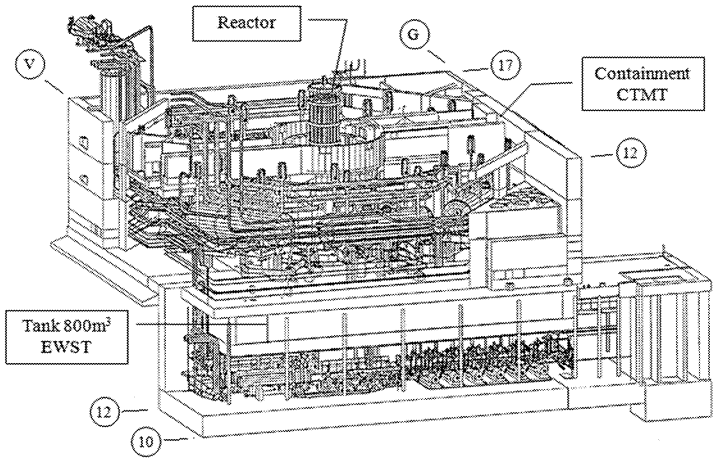

Fig.1: Containment and emergency tank 800 m^3 of NPP V1

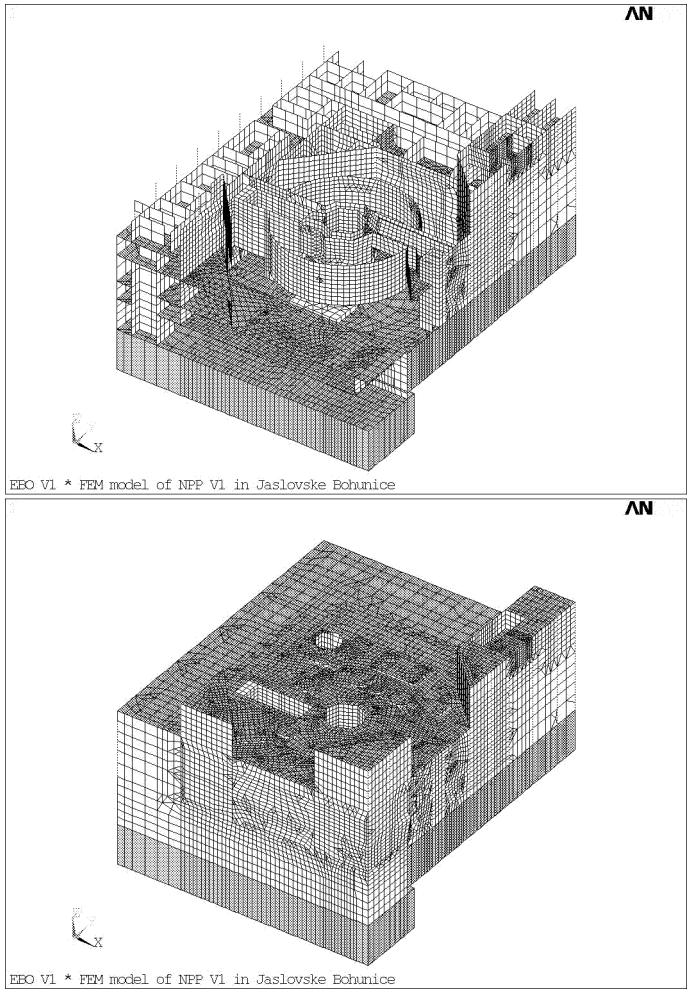

Fig.2: Computational model of the NPP building with layered shell elements

Králik) were provided to solve this task. The building of the power block was idealized with a discrete model consisting of 26 923 elements with 325 036 DOF. The link finite elements and the infinite layered space elements developed by the author [16] were used to model the soil. The link finite elements for the model of the thin soil layer under the power block building loaded by a steam pressure are accurate enough, and thus create a more realistic model. Recently the soil under the foundation plate has been consolidated.

The accident scenario was defined by SIEMENS KWU, VÚEZ Tlmače and VÚJE Trnava within the Phare program and 'The NPP V1 Reconstruction Project' [12].

2. Nonlinear solution of concrete cracking and crushing

The probabilistic analysis of the containment integrity failure is based on the nonlinear analysis of the concrete structures due to the accident of the coolant system and under the high level of the overpressure into the box of the steam generator.

The theory of large strain and rate independent plasticity were proposed during the high overpressure loading using the SHELL91 or the SHELL281 layered shell element from the ANSYS library [10 and 27].

The vector of the deformation parameters $\{r\}$ of this element (Figure 3) with the corner nodes '1, 2, 3, 4' and midside nodes '5, 6, 7, 8' is defined in the form

$$\{r\} = \{r_1, r_2, r_3, r_4, r_5, r_6, r_7, r_8\}^{\mathrm{T}} , \qquad \{r_i\} = \{u_{\mathrm{x}i}, u_{\mathrm{y}i}, u_{\mathrm{z}i}, \theta_{\mathrm{x}i}, \theta_{\mathrm{y}i}\}^{\mathrm{T}} \quad \forall i = 1, 8 . \tag{1}$$

The vector of the displacement of the l^{th} shell layer $\{u^l\} = \{u^l_{\mathrm{x}}, u^l_{\mathrm{y}}, u^l_{\mathrm{z}}\}^{\mathrm{T}}$ is approximated by the quadratic polynomial [10] in the form

$$\{u^l\} = \begin{Bmatrix} u^l_{\mathrm{x}} \\ u^l_{\mathrm{y}} \\ u^l_{\mathrm{z}} \end{Bmatrix} = \sum_{i=1}^{8} N_i \begin{Bmatrix} u_{\mathrm{x}i} \\ u_{\mathrm{y}i} \\ u_{\mathrm{z}i} \end{Bmatrix} + \sum_{i=1}^{8} N_i \frac{\zeta\, t_i}{2} \begin{bmatrix} a_{1,i} & b_{1,i} \\ a_{2,i} & b_{2,i} \\ a_{3,i} & b_{3,i} \end{bmatrix} \begin{Bmatrix} \theta_{\mathrm{x}i} \\ \theta_{\mathrm{y}i} \end{Bmatrix} , \tag{2}$$

where N_i is the shape function for i-node of the 8-node quadrilateral shell element, $u_{\mathrm{x}i}$, $u_{\mathrm{y}i}$, $u_{\mathrm{z}i}$ are the motion of i-node, ζ is the thickness coordinate, t_i is the thickness at i-node, $\{a\}$ is the unit vector in x direction, $\{b\}$ is the unit vector in plane of element and normal to $\{a\}$, $\theta_{\mathrm{x}i}$ or $\theta_{\mathrm{y}i}$ are the rotations of i-node about vector $\{a\}$ or $\{b\}$.

The linear strain vector $\{\varepsilon^l\}$ for the l^{th} layer is related to the nodal displacement vector by

$$\{\varepsilon^l\} = [B^l]\,\{u^l\} , \tag{3}$$

where $[B^l]$ is the strain-displacement matrix based on the element shape functions. In the case of the elastic state the stress-strain relations for the l^{th} layer are defined in the form

$$\{\sigma^l\} = [D^l_{\mathrm{e}}]\,\{\varepsilon^l\} , \tag{4}$$

where $\{\varepsilon^l\}^{\mathrm{T}} = \{\varepsilon_{\mathrm{x}}, \varepsilon_{\mathrm{y}}, \gamma_{\mathrm{xy}}, \gamma_{\mathrm{yz}}, \gamma_{\mathrm{zx}}\}$ and $\{\sigma^l\}^{\mathrm{T}} = \{\sigma_{\mathrm{x}}, \sigma_{\mathrm{y}}, \tau_{\mathrm{xy}}, \tau_{\mathrm{yz}}, \tau_{\mathrm{zx}}\}$ and the matrix of the material stiffness

$$[D^l_{\mathrm{e}}] = \begin{bmatrix} B^l\, E^l_{\mathrm{x}} & B^l\, \mu^l_{\mathrm{xy}}\, E^l_{\mathrm{x}} & 0 & 0 & 0 \\ B^l\, \mu^l_{\mathrm{xy}}\, E^l_{\mathrm{x}} & B^l\, E^l_{\mathrm{y}} & 0 & 0 & 0 \\ 0 & 0 & G^l_{\mathrm{xy}} & 0 & 0 \\ 0 & 0 & 0 & \dfrac{G^l_{\mathrm{yz}}}{k_{\mathrm{s}}} & 0 \\ 0 & 0 & 0 & 0 & \dfrac{G^l_{\mathrm{zx}}}{k_{\mathrm{s}}} \end{bmatrix} ,$$

where $B^l = E^l_y/[E^l_y - (\mu^l_{xy})^2\, E^l_x]$, E^l_x (versus E^l_y) is Young modulus of the l^{th} layer in the direction x (versus y), G^l_{xy}, G^l_{yz}, G^l_{zx} are shear moduli of the l^{th} layer in planes XY, YZ and ZX; k_s is the coefficient of the effective shear area ($k_s = 1 + 0.2\, A/(25\, t^2) \geq 1.2$), A is the element area, t is the element thickness.

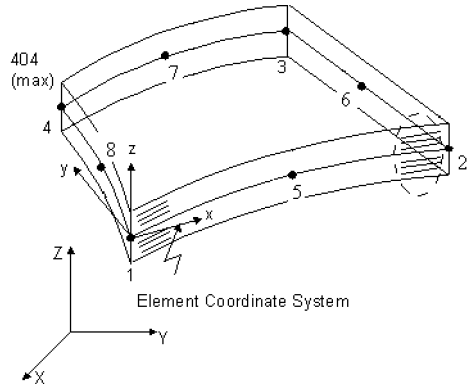

Fig.3: The shell element with 8 nodes

2.1. Geometric nonlinearity

If the rotations are large but the mechanical strains (those that cause stresses) are small, then a large rotation procedure can be used. A large rotation analysis is performed in a static analysis in the ANSYS program [10].

The strain in the n-step of the solution can be computed from the relations

$$\{\varepsilon_n\} = [B_o]\,[T_n]\,\{u_n\}\ , \tag{5}$$

where $\{u_n\}$ is the deformation displacement, $[B_o]$ is the original strain-displacement relationship, $[T_n]$ is the orthogonal transformation relating the original element coordinates to the convected (or rotated) element coordinates.

The convected element coordinate frame differs from the original element coordinate frame by the amount of rigid body rotation. Hence $[T_n]$ is computed by separating the rigid body rotation from the total deformation $\{u_n\}$ using the polar decomposition theorem. A corotational (or convected coordinate) approach is used in solving large rotation/small strain problems (Rankin and Brogan) [10].

2.2. Material nonlinearity

The presented constitutive model is a further extension of the smeared crack model [2, 5, 21 and 22], which was developed in [13]. Following the experimental results of Červenka, Kupfer, Jerga and Križma, and others [2, 9 and 18] a new concrete cracking layered finite shell element [13] was developed and incorporated into the ANSYS system [12, 13, 16 and 17]. The layered approximation and the smeared crack model of the shell element are proposed.

The processes of the concrete cracking and crushing are developed during the increasing of the load. The concrete compressive stress f_c, the concrete tensile stress f_t and the shear modulus G are reduced after the crushing or cracking of the concrete [2].

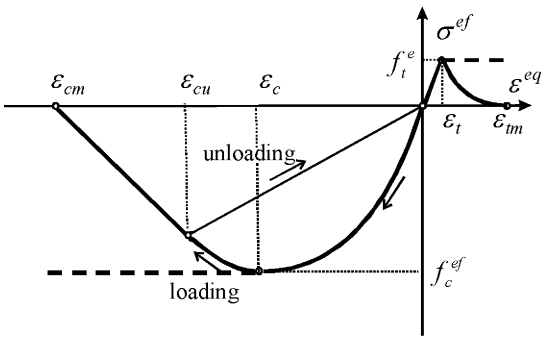

Fig.4: The concrete stress-strain diagram

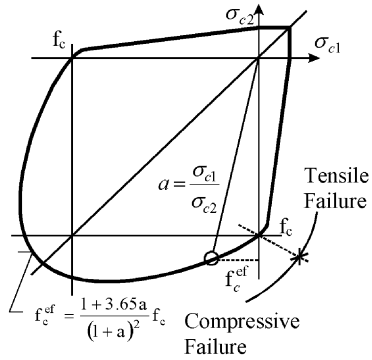

Fig.5: Kupfer's plasticity function

In this model the stress-strain relation is defined (Figure 4) following ENV 1992-1-1 (1991) [3]:

– Loading in the compression region $\varepsilon_{\rm cu} < \varepsilon^{\rm eq} < 0$

$$\sigma_{\rm c}^{\rm ef} = f_{\rm c}^{\rm ef}\,\frac{k\,\eta - \eta^2}{1+(k-2)\,\eta}\ , \qquad \eta = \frac{\varepsilon^{\rm eq}}{\varepsilon_{\rm c}}\ , \qquad (\varepsilon_{\rm c} \doteq -0.0022,\ \varepsilon_{\rm cu} \doteq -0.0035)\ . \tag{6}$$

– Softening in the compression region $\varepsilon_{\rm cm} < \varepsilon^{\rm eq} < \varepsilon_{\rm cu}$

$$\sigma_{\rm c}^{\rm ef} = f_{\rm c}^{\rm ef}\left(1 - \frac{\varepsilon^{\rm eq} - \varepsilon_{\rm c}}{\varepsilon_{\rm cm} - \varepsilon_{\rm cu}}\right)\ . \tag{7}$$

– The tension region $\varepsilon_{\rm t} < \varepsilon^{\rm eq} < \varepsilon_{\rm m}$

$$\sigma_{\rm c}^{\rm ef} = f_{\rm t}\,\exp\left[-2\,\frac{\varepsilon^{\rm eq} - \varepsilon_{\rm t}}{\varepsilon_{\rm tm}}\right] \qquad (\varepsilon_{\rm t} \doteq 0.0001,\ \varepsilon_{\rm tm} \doteq 0.002)\ . \tag{8}$$

In the case of the plane state the strength function in tension $f_{\rm t}$ and in compression $f_{\rm c}$ were considered equivalent values $f_{\rm t}^{\rm eq}$ and $f_{\rm c}^{\rm eq}$.

In the plane of principal stresses ($\sigma_{\rm c1},\ \sigma_{\rm c2}$) the relation between the one and bidimensional stresses state due to the plasticity function by Kupfer (see Figure 5) can be defined as follows:

– Compression-compression

$$f_{\rm c}^{\rm ef} = \frac{1+3.65\,a}{(1+a)^2}\,f_{\rm c}\ , \qquad a = \frac{\sigma_{\rm c1}}{\sigma_{\rm c2}}\ . \tag{9}$$

– Tension-compression

$$f_{\rm c}^{\rm ef} = f_{\rm c}\,r_{\rm ec}\ , \qquad r_{\rm ec} = 1 + 5.3278\,\frac{\sigma_{\rm c1}}{f_{\rm c}}\ , \qquad r_{\rm ec} \geq 0.9\ . \tag{10}$$

– Tension-tension

$$f_{\rm t}^{\rm ef} = f_{\rm t}\,r_{\rm et}\ , \qquad r_{\rm et} = \frac{A+(A-1)\,B}{A\,B}\ , \qquad B = K\,x + a\ , \qquad x = \frac{\sigma_{\rm c2}}{f_{\rm c}}\ , \tag{11}$$
$$r_{\rm et} = 1 \Leftrightarrow x = 0\ , \quad r_{\rm et} = 0.2 \Leftrightarrow x = 1\ .$$

The shear concrete modulus G was defined for cracking concrete by Kolmar [11] in the form

$$G = r_{\mathrm{g}}\, G_{\mathrm{o}}\ , \quad r_{\mathrm{g}} = \frac{1}{c_2}\ \ln\frac{\varepsilon_{\mathrm{u}}}{c_1}\ , \quad c_1 = 7 + 333\,(p - 0.005)\ , \quad c_2 = 10 - 167\,(p - 0.005)\ , \tag{12}$$

where G_{o} is the initial shear modulus of concrete, ε_{u} is the strain in the normal direction to crack, c_1 and c_2 are the constants dependent on the ratio of reinforcing, p is the ratio of reinforcing transformed to the plane of the crack ($0 < p < 0.02$).

It is proposed that the crack in the one layer of shell element is oriented perpendicular to the orientation of principal stresses. The membrane stress and strain vector depends on the direction of the principal stress and strain in one layer

$$\{\varepsilon_{\mathrm{cr}}\} = [T_\varepsilon]\,\{\varepsilon\}\ , \qquad \{\sigma_{\mathrm{cr}}\} = [T_\sigma]\,\{\sigma\}\ , \tag{13}$$

where $[T_\varepsilon]$, $[T_\sigma]$ are transformation matrices for the principal strain and stress in the direction θ in the layer.

$$[T_\varepsilon] = \begin{bmatrix} \cos^2\theta & \sin^2\theta & \sin\theta\,\cos\theta & 0 & 0 \\ \sin^2\theta & \cos^2\theta & -\sin\theta\,\cos\theta & 0 & 0 \\ -2\,\sin\theta\,\cos\theta & 2\,\sin\theta\,\cos\theta & \cos 2\theta & 0 & 0 \\ 0 & 0 & 0 & \cos\theta & \sin\theta \\ 0 & 0 & 0 & -\sin\theta & \cos\theta \end{bmatrix}\ ,$$
$$[T_\sigma] = \begin{bmatrix} \cos^2\theta & \sin^2\theta & 2\,\sin\theta\,\cos\theta & 0 & 0 \\ \sin^2\theta & \cos^2\theta & -2\,\sin\theta\,\cos\theta & 0 & 0 \\ -\sin\theta\,\cos\theta & \sin\theta\,\cos\theta & \cos 2\theta & 0 & 0 \\ 0 & 0 & 0 & \cos\theta & \sin\theta \\ 0 & 0 & 0 & -\sin\theta & \cos\theta \end{bmatrix}\ . \tag{14}$$

The strain-stress relationship in the Cartesian coordinates can be defined in dependency on the direction of the crack (in the direction of principal stress, versus strain)

$$[\sigma_{\mathrm{cr}}] = [D_{\mathrm{cr}}]\,\{\varepsilon_{\mathrm{cr}}\} \quad \text{and therefore} \quad [\sigma] = [T_\sigma]^{\mathrm{T}}\,[D_{\mathrm{cr}}]\,[T_\varepsilon]\,\{\varepsilon\}\ . \tag{15}$$

For the membrane and bending deformation of the reinforced concrete shell structure the layered shell element, on which a plane state of stress is proposed on every single layer, was used.

The stiffness matrix of the reinforced concrete for the l^{th} layer can be written in the following form

$$[D^l_{\mathrm{cr}}] = [T^l_{\mathrm{c}\sigma}]^{\mathrm{T}}\,[D^l_{\mathrm{cr}}]\,[T^l_{\mathrm{c}\varepsilon}] + \sum_{s=1}^{Nrein} [T^l_s]^{\mathrm{T}}\,[D^l_s]\,[T^l_s]\ , \tag{16}$$

where $[T_{\mathrm{c}\sigma}]$, $[T_{\mathrm{c}\varepsilon}]$, $[T_s]$ are the transformation matrices for the concrete and the reinforcement separately, $Nrein$ is the number of the reinforcements in the l^{th} layer.

After cracking the elasticity modulus and Poisson's ratio are reduced to zero in the direction perpendicular to the cracked plane, and a reduced shear modulus is employed.

Considering 1 and 2 two principal directions in the plane of the structure, the stress-strain relationship for the concrete l^{th} layer cracked in the 1-direction, is

$$\left\{\begin{array}{c}\sigma_1\\ \sigma_2\\ \tau_{12}\\ \tau_{13}\\ \tau_{23}\end{array}\right\}_l = \left[\begin{array}{ccccc}0 & 0 & 0 & 0 & 0\\ 0 & E & 0 & 0 & 0\\ 0 & 0 & G_{12}^{\text{cr}} & 0 & 0\\ 0 & 0 & 0 & G_{13}^{\text{cr}} & 0\\ 0 & 0 & 0 & 0 & G_{23}^{\text{cr}}\end{array}\right]_l \left\{\begin{array}{c}\varepsilon_1\\ \varepsilon_2\\ \gamma_{12}\\ \gamma_{13}\\ \gamma_{23}\end{array}\right\}_l , \tag{17}$$

where the shear moduli are reduced by the coefficient of the effective shear area k_{s} and parameter r_{g1} by Kolmar (12) as follows: $G_{12}^{\text{cr}} = G_{\text{o}}\, r_{\text{g1}}$, $G_{13}^{\text{cr}} = G_{\text{o}}\, r_{\text{g1}}$, $G_{23}^{\text{cr}} = G_{\text{o}}/k_{\text{s}}$.

When the tensile stress in the 2-direction reaches the value f_{t}', the latter cracked plane perpendicular to the first one is assumed to form, and the stress-strain relationship becomes:

$$\left\{\begin{array}{c}\sigma_1\\ \sigma_2\\ \tau_{12}\\ \tau_{13}\\ \tau_{23}\end{array}\right\}_l = \left[\begin{array}{ccccc}0 & 0 & 0 & 0 & 0\\ 0 & 0 & 0 & 0 & 0\\ 0 & 0 & G_{12}^{\text{cr}}/2 & 0 & 0\\ 0 & 0 & 0 & G_{13}^{\text{cr}} & 0\\ 0 & 0 & 0 & 0 & G_{23}^{\text{cr}}\end{array}\right]_l \left\{\begin{array}{c}\varepsilon_1\\ \varepsilon_2\\ \gamma_{12}\\ \gamma_{13}\\ \gamma_{23}\end{array}\right\}_l , \tag{18}$$

where the shear moduli are reduced by the parameter r_{g1} and r_{g2} by Kolmar (12) as follows: $G_{12}^{\text{cr}} = G_{\text{o}}\, r_{\text{g1}}$, $G_{13}^{\text{cr}} = G_{\text{o}}\, r_{\text{g1}}$, $G_{23}^{\text{cr}} = G_{\text{o}}\, r_{\text{g2}}$.

The cracked concrete is anisotropic and these relations must be transformed to the reference axes XY. The simplified averaging process is more convenient for finite element formulation than the singular discrete model. A smeared representation for the cracked concrete implies that cracks are not discrete but distributed across the region of the finite element.

The smeared crack model [21 and 22], used in this work, results from the assumption, that the field of more micro cracks (not one local failure) brought to the concrete element will be created. The validity of this assumption is determined by the size of the finite element, hence its characteristic dimension $L_{\text{c}} = \sqrt{A}$, where A is the element area (versus integrated point area of the element). For the expansion of cracking the assumption of constant failure energies $G_{\text{f}} = \text{const}$ is proposed in the form

$$G_{\text{f}} = \int_0^{\infty} \sigma_{\text{n}}(w)\, \text{d}w = A_{\text{G}}\, L_{\text{c}} , \qquad w_{\text{c}} = \varepsilon_{\text{w}}\, L_{\text{c}} , \tag{19}$$

where w_{c} is the width of the failure, σ_{n} is the stress in the concrete in the normal direction, A_{G} is the area under the stress-strain diagram of concrete in tension. Concrete modulus for descend line of stress strain diagram in tension (crushing) can be described according to Oliver [22] in dependency on the failure energies in the form

$$E_{\text{c,s}} = \frac{E_{\text{c}}}{1 - \lambda_{\text{c}}} , \qquad \lambda_{\text{c}} = \frac{2\, G_{\text{f}}\, E_{\text{c}}}{L_{\text{c}}\, \sigma_{\text{max}}^2} , \tag{20}$$

where E_{c} is the initial concrete modulus elasticity, σ_{max} is the maximal stress in the concrete tension. From the condition of the real solution of the relation (20) it follows, that the characteristic dimension of element must satisfy the following condition

$$L_{\text{c}} \leq \frac{2\, G_{\text{f}}\, E_{\text{c}}}{\sigma_{\text{max}}^2} . \tag{21}$$

The characteristic dimension of the element is determined by the size of the failure energy of the element. The theory of a concrete failure was implied and applied to the 2D layered shell elements SHELL91 and SHELL281 in the ANSYS element library [17].

The limit of damage at a point is controlled by the values of the so-called crushing or total failure function F_{u}. The modified Kupfer's condition [18] for the l^{th} layer of section is following

$$F_{\mathrm{u}}^{l} = F_{\mathrm{u}}^{l}(I_{\varepsilon 1}; J_{\varepsilon 2}; \varepsilon_{\mathrm{u}}) \ , \qquad F_{\mathrm{u}}^{l} = \sqrt{\beta\,(3\,J_{\varepsilon 2}) + \alpha\,I_{\varepsilon 1}} - \varepsilon_{\mathrm{u}} = 0 \ , \tag{22}$$

where $I_{\varepsilon 1}$, $J_{\varepsilon 2}$ are the strain invariants, and ε_{u} is the ultimate total strain extrapolated from uniaxial test results ($\varepsilon_{\mathrm{u}} = 0.002$ in the tension domain, or $\varepsilon_{\mathrm{u}} = 0.0035$ in the compression domain), α, β are the material parameters determined from the Kupfer's experiment results ($\beta = 1.355$, $\alpha = 0.355\,\varepsilon_{\mathrm{u}}$) [18 and 22].

The failure function of the whole section will be obtained by the integration of the failure function through to the whole section in the form

$$F_{\mathrm{u}} = \frac{1}{t}\int_{0}^{t} F_{\mathrm{u}}^{l}\,(I_{\varepsilon 1}; J_{\varepsilon 2}; \varepsilon_{\mathrm{u}})\,\mathrm{d}z = \frac{1}{t}\sum_{l=1}^{Nlay} F_{\mathrm{u}}^{l}\,(I_{\varepsilon 1}; I_{\varepsilon 2}; \varepsilon_{\mathrm{u}})\,t_{l} \ , \tag{23}$$

where t_l is the thickness of the l^{th} shell layer, t is the total shell thickness and $Nlay$ is the number of layers. This failure condition is determined by the maximum strain ε_{s} of the reinforcement steel in the tension area ($\max(\varepsilon_{\mathrm{s}}) \le \varepsilon_{\mathrm{sm}} = 0.01$) and by the maximum concrete crack width w_{c} ($\max(w_{\mathrm{c}}) \le w_{\mathrm{cm}} = 0.3\,\mathrm{mm}$).

3. Degradation of a reinforced concrete structure

The safety of nuclear power plants could be affected by the age related degradation of structures [1] if it is not detected prior to the loss of the functional capability and if timely corrective action is not taken.

The reduction even or the loss of functional capability of the key plant components could reduce the plant safety. Mild steel reinforcing bars are provided to control the extent of cracking and the width of cracks at operating temperatures, to resist tensile stresses and computed compressive stresses for elastic design, and to provide the structural reinforcement where required. Potential causes of degradation of the reinforcing steel would be corrosion, exposure to elevated temperatures and irradiation [1, 20, 25 and 27].

So-called 'uniform' or general corrosion consists of approximately uniform loss of metal over the whole exposed surface of the reinforcing bar [1]. Faraday's law indicates that a corrosion current density of $i_{\mathrm{corr}} = 1\,\mu\mathrm{A\,cm^{-2}}$ corresponds to a uniform corrosion penetration of $11.6\,\mu\mathrm{m\,year^{-1}}$. Thus the reduction of the diameter of a corroding bar, ΔD, at time T, can be estimated directly (in mm) from i_{corr} as

$$\Delta D(T) = 0.0232\int_{T_{\mathrm{o}}}^{T} i_{\mathrm{corr}}(t)\,\mathrm{d}t \ , \tag{24}$$

where T is the actual time, T_{o} is the time of corrosion initiation (in years). If a constant annual corrosion rate is assumed, equation (24) reduces to the following equation

$$\Delta D(T) = 0.0232\,(T - T_{\mathrm{o}})\,i_{\mathrm{corr}} \ .$$

The net cross-sectional area of a reinforcing bar, A_{r} at time T, is then equal to

$$A_{\mathrm{r}}(T) = \begin{cases} \dfrac{\pi\, D_{\mathrm{o}}^2}{4} & T \leq T_{\mathrm{o}}\ , \\ \dfrac{\pi\, [D_{\mathrm{o}} - \Delta D(T)]^2}{4} & T > T_{\mathrm{o}}\ , \end{cases} \tag{25}$$

where D_{o} is the initial diameter of the reinforcing bar (in mm).

The limit concrete strength and its Young modulus are practically not changed during the corrosion process. The corrosion process can be considered as the reduction of the reinforced steel cross section. The state of the NPP reinforced concrete structures has been periodically monitored in the frame of the IAEA requirements for safety and reliability of the NPP performance.

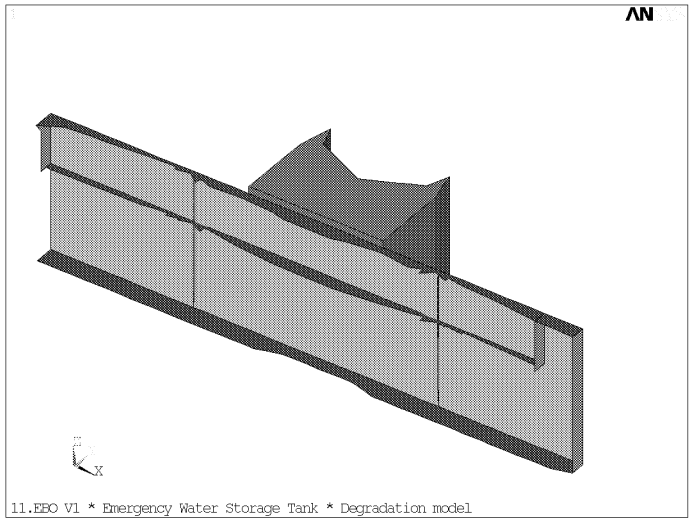

Fig.6: Computational model with two vertical cracks

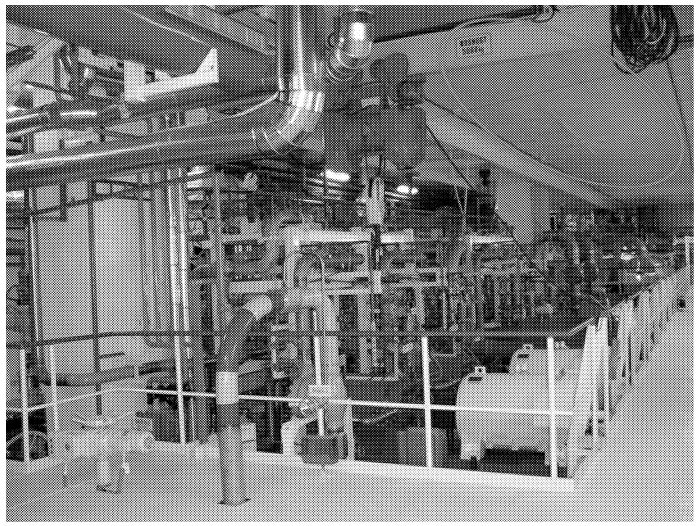

Fig.7: Degradation effects at the basin bottom

Special attention was paid to the EWST structure. After 10 years of the operation, two vertical cracks in the wall in axis 12, near the contact of the reactor corps and the basin wall, were identified (Figure 6). Also, hence the degradation effects at the bottom of the emergency water storage tank were identified (Figure 7). These effects were the consequence of the corrosion process of the reinforced steel in the basin plate.

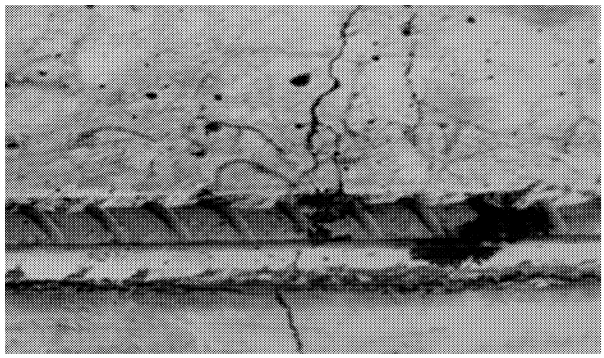

Fig.8: Detail of reinforcement and the concrete crack

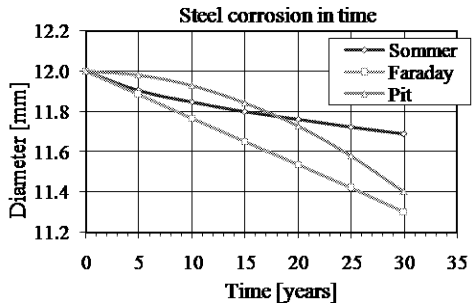

Fig.9: Steel corrosion depending on time

There is proposed conservatively that this corrosion process had been acting from 10 to 20 years. In regard to all uncertainties to define the influence of the corrosion effects and to identify cracks the state of the NPP structure resistance is investigated using the probabilistic methodology and conservative proposition of the degradation processes.

The corrosion effects of the reinforcement at the basin bottom and in the concrete cracks (Figure 8) were considered according to Faraday's law (Figure 9) using the uniform corrosion penetration (of $11.6\,\mu\mathrm{m\,year}^{-1}$). This assumption is also conservative from the point of view of the higher safety level [1].

4. Nonlinear deterministic analysis

The critical sections of the structure were determined on the base of the nonlinear analysis due to the monotone increasing of overpressure inside the hermetic zone [12 and 13]. The resistance of these critical sections was considered taking into account the design values of the material characteristics and the load. The combination load and design criteria were considered for the BDBA state [16].

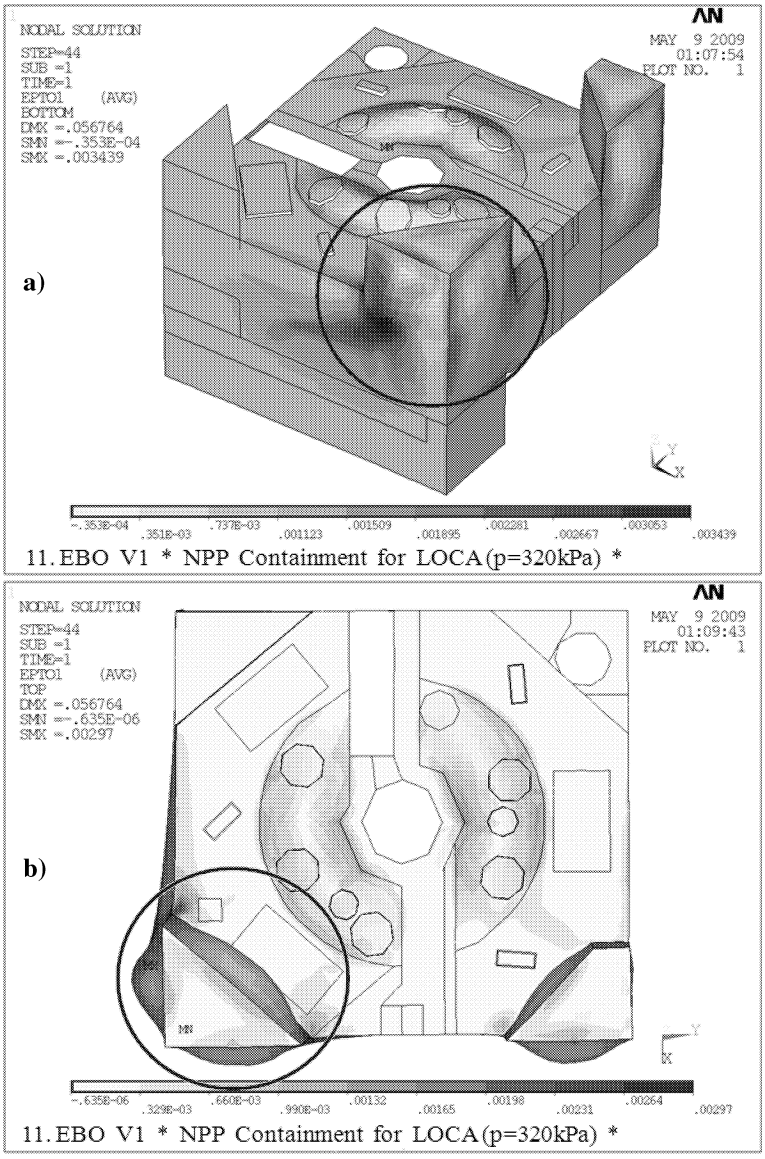

Fig.10: Critical area of containment structure loading at overpressure 320 kPa

The critical areas were identified in the connection walls and plate of the hermetic zone at level +10.5 m near the hole in the modulus '10' and 'V' (Figure 10). The tension forces and the bending moments were concentrated between two outside large walls.

On the base of the nonlinear analysis of the containment resistance for median values of the material properties and failure function (22) the critical overpressure was equal to 309 kPa without the degradation effect and 287 kPa (versus 283 kPa) with degradation effects during 10 years (versus 20 years) (Figure 11a).

The capacity of the concrete wall of the EWST structure is equal 45 % without considering the degradation effect (versus 50 % with the degradation effect after 20 years) under overpressure 300 kPa in the CTMT structure (Figure 11b). The temperature of the water

(about 55 °C) in the emergency tank (EWST) affects the compression in the tank wall as the prestressed. This effect is opposite to the overpressure effects in the CTMT. The degradation effect occurs during overpressure higher than 150 kPa (Figure 11).

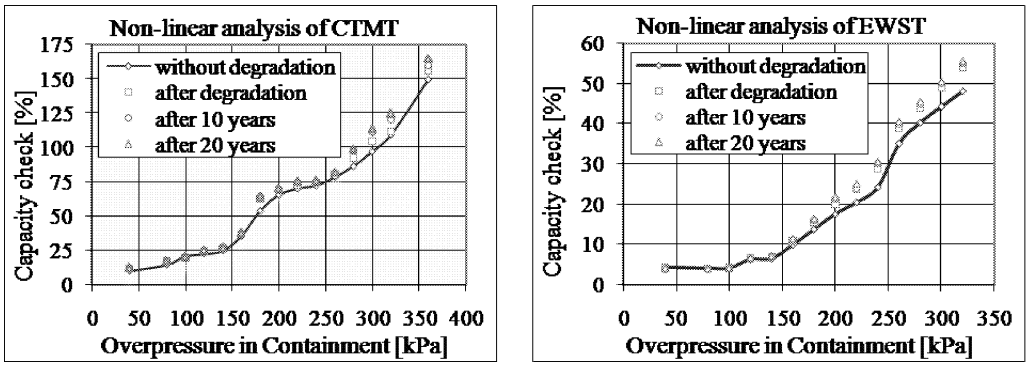

Fig.11: The capacity utilization of the reinforced concrete containment (CTMT) and emergency water storage tank (EWST) due to overpressure with and without degradation effects

5. Probabilistic analysis of the structure reliability

Recent advances and the general accessibility of information technologies and computing techniques give rise to assumptions concerning the wider use of the probabilistic assessment of the reliability of structures through the use of simulation methods in the Czech Republic and Slovakia [6, 14, 15, 16, 17, 25 and 26]. A great attention should be paid to using the probabilistic approach in an analysis of the reliability of structures [4, 8, 19, 20, 23 and 26].

Most problems concerning the reliability of building structures are defined today as a comparison of two stochastic values, loading effects E and the resistance R, depending on the variable material and geometric characteristics of the structural element. The variability of those parameters is characterized by the corresponding functions of the probability density $f_{\mathrm{R}}(r)$ and $f_{\mathrm{E}}(e)$. In the case of a deterministic approach to the design the deterministic (nominal) attributes of those parameters R_{d} and E_{d} are compared.

The deterministic definition of the reliability condition is of the form

$$R_{\mathrm{d}} \geq E_{\mathrm{d}} \tag{26}$$

and in the case of the probabilistic approach it is of the form

$$RF = g(R, E) = R - E \geq 0 \ , \tag{27}$$

where $g(R, E)$ is the reliability function.

The probability of failure can be defined by the simple expression

$$P_{\mathrm{f}} = P[R < E] = P[(R - E) < 0] \ . \tag{28}$$

The reliability function RF can be expressed generally as a function of the stochastic parameters X_1, X_2 to X_n, used in the calculation of R and E.

$$RF = g(X_1, X_2, \ldots, X_n) \ . \tag{29}$$

The failure function $g(\{X\})$ represents the condition (reserve) of the reliability, which can be either an explicit or implicit function of the stochastic parameters and can be single (defined on one cross-section) or complex (defined on several cross-sections, e.g., on a complex finite element model).

In the case of simulation methods the failure probability is calculated from the evaluation of the statistical parameters and theoretical model of the probability distribution of the reliability function $Z = g(X)$. The failure probability is defined as the best estimation on the base of numerical simulations in the form

$$p_{\mathrm{f}} = \frac{1}{N} \sum_{i=1}^{N} I[g(X_i) \leq 0] \ , \tag{30}$$

where N in the number of simulations, $g(.)$ is the failure function, $I[.]$ is the function with value 1, if the condition in the square bracket is fulfilled, otherwise is equal 0.

The RSM method was chosen for the PSA analysis of the containment safety. It is based on the assumption that it is possible to define the dependency between the variable input and the output data through the approximation functions in the following form:

$$Y = c_{\mathrm{o}} + \sum_{i=1}^{N} c_i \, X_i + \sum_{i=1}^{N} c_{ii} \, X_i^2 + \sum_{i=1}^{N-1} \sum_{j=i+1}^{N} c_{ij} \, X_i \, X_j \ , \tag{31}$$

where c_{o} is the index of the constant member; c_i are the indices of the linear member and c_{ij} the indices of the quadratic member, which are given for predetermined schemes for the optimal distribution of the variables or for using the regression analysis after calculating the response. Approximate polynomial coefficients are given from the condition of the error minimum, usually by the 'Central Composite Design Sampling' (CCD) method or the 'Box-Behnken Matrix Sampling' (BBM) method [10].

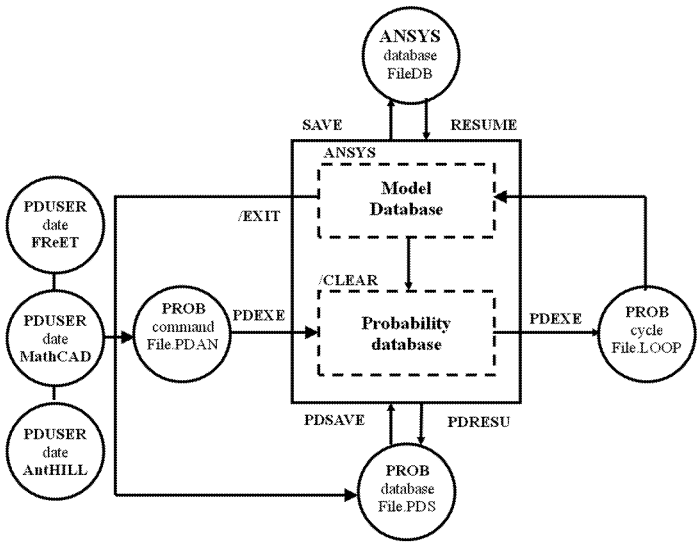

Fig.12: A procedural diagram of the probabilistic calculations using the ANSYS software system

The computation efficiency of the experimental design depends on the number of design points, which must be at least equal to the number of the unknown coefficients. In the classical design approach, a regression analysis is carried out to formulate the response surface after calculating the responses at the sampling points. These points should have at least 3 levels for each variable to fit the second-order polynomial, leading to 3^k factorial design. This design approach becomes inefficient with the increasing of the number of random variables. More efficient is the central composite design, which was developed by Box and Wilson [10].

The central CCD method is composed of (Figure 13a):

1. Factorial portion of design – a complete 2^k factorial design (equal -1, $+1$),
2. Center point – n_o center points, $n_o \geq 1$ (generally $n_o = 1$),
3. Axial portion of design – two points on the axis of each design variable at distance α from the design center.

Then the total number of design points is $N = 2^k + 2\,k + n_o$, which is much more than the number of the coefficients $p = (k+1)(k+2)/2$. The graphical representation for $k = 3$ and the matrix form of the coded values are represented in Figure 13.

It is advisable to use the displacement-based FEM for reliability analysis of the complicated structures with one of the defined simulation methods. In this work the ANSYS licensed program [10] with a probabilistic postprocessor was utilized for the probability analysis of the reliability of the NPP structures for various action effects. In Figure 13, the procedural diagram sequence is presented from the structure of the model through the calculations, up to the evaluation of the probability of the structural failure.

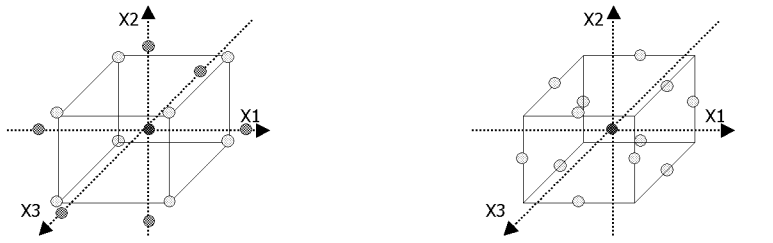

a) The Central Composite Design b) The Box-Behnken Matrix Design

Fig.13: Distribution schemes of the stochastic numbers of the RSM method for three input variables

The postprocessor for the probabilistic design of structures enables to define the random variables using the standard distribution functions (normal, lognormal, exponential, beta, gamma, weibull, etc.), or externally (user-defined sampling) using other statistical programs as the AntHILL or the FREET. The probabilistic calculation procedures are based on the Monte Carlo simulations (DS, LHS, user-defined sampling) and the approximation RSM method (CCD, BBM, user-defined sampling) [15 and 17]. The RSM method generates the explicit performance function for the implicit or complicated limit state function. This method is very effective for robust and complicated tasks.

On the base of experimental design, the unknown coefficients are determined due to the random variables selected within the experimental region. The uncertainty in the random variables can be defined in the model by varying in the arbitrary amount producing the whole experimental region.

6. PSA level 3 analysis of containment failure

The methodology of the probabilistic analysis of integrity of reinforced concrete structures of containment results from requirements [8] and experience from their applications [14, 15, 16, 19, 25 and 26].

The probability of containment failure is calculated from the probability of the reliability function RF in the form

$$P_{\mathrm{f}} = P(RF < 0) \ , \tag{32}$$

where the reliability condition RF is defined depending on a concrete failure condition (30)

$$RF = -F_{\mathrm{u}}(I_{\varepsilon 1}; J_{\varepsilon 2}; \varepsilon_{\mathrm{u}}) \ , \tag{33}$$

where the failure function $F_{\mathrm{u}}(.)$ was considered in the form (23).

The previous design analyses, calculations and additions include various uncertainties, which determine the results of probability bearing analysis of containment structural integrity are presented in Table 1. Due to the mentioned uncertainties of the input data for the probabilistic analysis of reinforced concrete containment structures loss of integrity the mean values and standard deviations, the variable parameters for normal, lognormal and beta distribution were determined.

	Soil	Material	Loads				Model	
	Stiffness	Young modulus	Dead load	Live load	Pressure	Temperature	Action uncertaint	Resist. uncertaint
Characteristic value	kz_k	E_k	G_k	Q_k	P_k	T_k	Te_k	Tr_k
Variable	kz_{var}	e_{var}	g_{var}	q_{var}	p_{var}	t_{var}	Te_{var}	Tr_{var}
Histogram type	N	LN	N	BETA	N	BETA	N	N
Mean value μ	1	1	1	0.643	1	0.933	1	1
Deviation σ [%]	5	11.1	10	22.6	8	14.1	5	5
Minimum value	0.754	0.649	0.621	0.232	0.662	0.700	0.813	0.813
Maximum value	1.192	1.528	1.376	1.358	1.301	1.376	1.206	1.206

Tab.1: Variable parameters of the input data

On the base of the RSM simulations the increment vector of the deformation parameters $\{\Delta r_s\}$ in the FEM is defined for the s^{th} simulation in the form

$$\{\Delta r_s\} = [K_{\mathrm{GN}}(E_s, kz_s, F_\sigma)]^{-1} \{\Delta F(G_s, Q_s, P_s, T_s)\} \tag{34}$$

and the strain vector increment

$$\{\Delta \varepsilon_s\} = [B_s] \{\Delta r_s\} \ , \tag{35}$$

where $[K_{\mathrm{GN}}]$ is the nonlinear stiffness matrix depending on the variable parameters E_s, kz_s and F_σ, F_σ is the Kupfer's yield function defined in the stress components, $\{\Delta F\}$ is the increment vector of the general forces depending on the variable parameters G_s, Q_s, P_s and T_s for the s^{th} simulation. The total strain vector is defined as the sum of the strain increments

$$\{\varepsilon_s\} = \sum_{istep=1}^{Nstep} \{\Delta \varepsilon_s\}_{istep} \ . \tag{36}$$

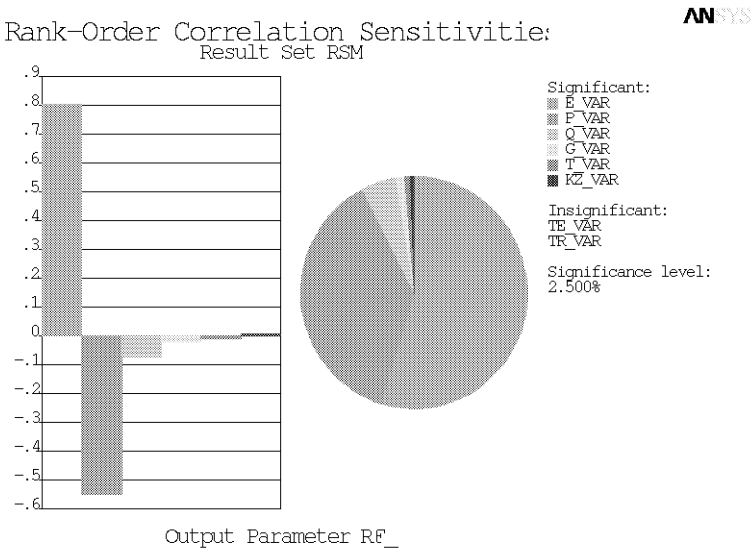

a) 10.EBO V1 * NPP Containment for LOCA (p=320kPa) *

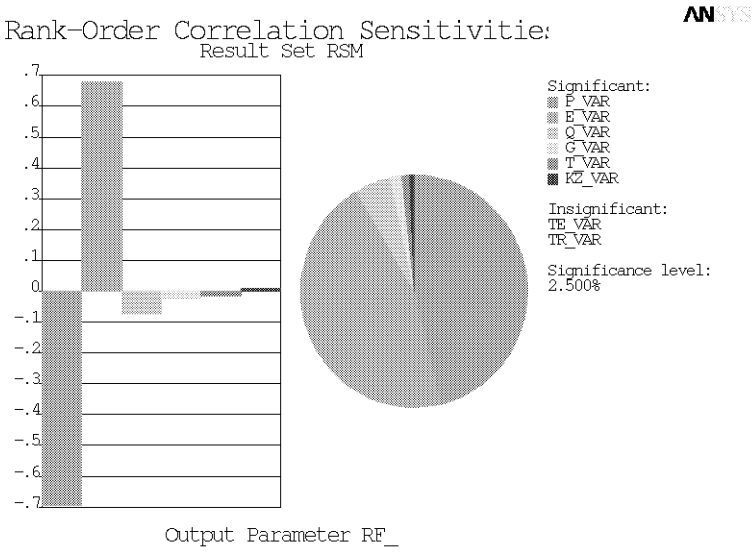

b) 11.EBO V1 * NPP Containment for LOCA (p=320kPa) *

Fig.14: Sensitivity of reliability function RF

Resulting from the variability of the input quantity 25 simulation steps on the base of the RSM method under the ANSYS-CRACK system were realized [16]. The probability of loss containment structure integrity was calculated from 10^6 Monte Carlo simulations for 25 steps of the RSM approximation method on the full structural FEM model. The probability analysis was considered for the structural model without (model V1_10) and with (model V1_11) the wall cracking and the corrosion effects below the emergency tank (Figure 1).

The evaluation of the probabilistic sensitivities was calculated from the correlation coefficients between all random input variables and a particular random output parameter by

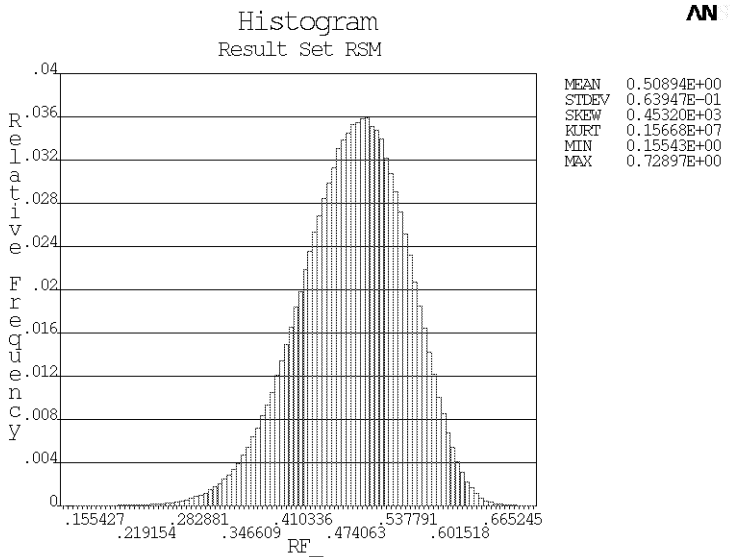

a) 10.EBO V1 * NPP Containment for LOCA (p=320kPa) *

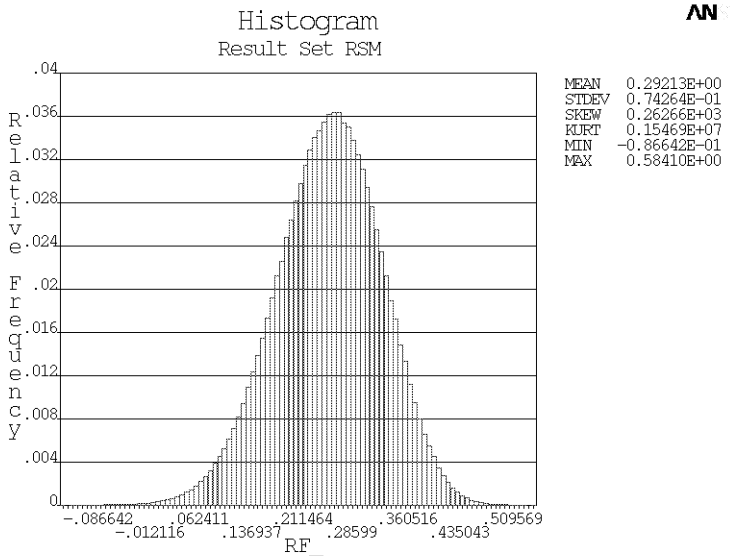

b) 11.EBO V1 * NPP Containment for LOCA (p=320kPa) *

Fig.15: Reliability function RF under overpressure 320 kPa for two models: a) without the degradation effect, b) with the degradation effect

Spearman [10]. These analyses show (Figure 14) that the variability of the overpressure and the structure stiffness have the fundamental impact upon the reliability of the containment. The effects of the variability of the concrete stiffness are dominant in the model V1_10 without the degradation effect (Figure 14a), and on the other hand, the variability of the overpressure is dominant in the model V1_11 with the degradation effect (Figure 14b).

The probability of the concrete structure failure in accordance with the relation (33) under overpressure 320 kPa is less than 10^{-6} in the model without cracking effects (original status). If the influence of the tank wall cracking and the corrosion effects are considered the probability of failure is equal 1.375×10^{-4} for overpressure 320 kPa. The histograms of

the reliability function RF under overpressure 320 kPa for two models without (V1_10) and with (V1_11) the degradation effect, respectively, are presented in Figure 15.

7. Conclusion

The probability analysis of the loss of the concrete containment integrity was made for the overpressure loads from 40 kPa to 320 kPa using the nonlinear solution of the static equilibrium considering the geometric and material nonlinearities of the reinforced concrete shell layered elements. The nonlinear analyses were performed in the CRACK program, which was developed by the author and implemented into the ANSYS system [12 and 13]. The uncertainties of the loads level (longtime temperature and dead loads), the material model of the composite structure (concrete cracking and crushing, reinforcement, and liner), the degradation effects (carbonization and reinforcement corrosion) and other influences following from the inaccuracy of the calculated model and the numerical methods were taken into account in the MONTE CARLO simulations on the base of the RSM method [16 and 17]. The reliability function RF was defined in dependency on the failure function $F_{\mathrm{u}}(I_{\varepsilon 1}; J_{\varepsilon 2}; \varepsilon_{\mathrm{u}})$ for requirements of the PSA analysis in the form (23). The probability of the loss of the concrete containment integrity is less than 10^{-6} for the original structural model. In the case of the degradation effects of the concrete structure under the emergency tank the probability of the containment failure is equal to 1.375×10^{-4} for the overpressure 320 kPa. The theory of the nonlinear analysis using the RSM method was developed in the framework of the VEGA grant project [16 and 17].

Acknowledgement

The project was performed with the financial support of the Grant Agency of the Slovak Republic (VEGA). The project registration number is VEGA 1/0849/08.

References

[1] ACI Committee E 222, Corrosion of Metals in Concrete, ACI 222R-89, American Concrete Institute 1989, Detroit, MI
[2] Červenka V.: Constitutive Model for Cracked Reinforced Concrete, ACI Journal 82 (1985) 877
[3] Eurocode 2, Design of Concrete Structures, Part 1, CEC 1990
[4] Haldar A., Mahadevan S.: Probability, Reliability and Statistical Methods in Engineering Design, John Wiley & Sons 2000, New York
[5] Hinton E., Owen D. R. J.: Finite Element Software for Plates and Shells, DCE University College Swansea U. K., Pineridge Press 1984, Swansea
[6] Holický M., Marková J.: Base of reliability theory and risk evaluation, ČVUT Praha 2005, Praha (in Czech)
[7] Hughes T.J.R.: Numerical Implementation of Constitutive Models: Rate-Independent Deviatoric Plasticity, Theoretical Foundation for Large-Scale Computations for Nonlinear Material Behavior, eds. S. Nemat-Nasser, R.J. Asaro, G.A. Hegemier, Martinus Nijhoff Publishers 1984, Dordrecht
[8] IAEA: Development and Application of Level 2 Probabilistic Safety Assessment for Nuclear Power Plants, Draft Safety Guide DS393, Draft 6, 2008
[9] Jerga J., Križma M.: Assessment of Concrete Damage, Building Research Journal 54 (2006) 211
[10] Kohnke P.: ANSYS, Theory, SAS IP Inc. 2008, Canonsburg
[11] Kolmar W.: Beschreibung der Kraftuebertragung ueber Risse in nichtlinearen Finite-Element-Berechnungen von Stahlbetontragwerken, PhD Thesis, T. H. Darmstadt 1986, Darmstadt

[12] Králik J.: Experimental and Numerical Analysis of Reinforced Concrete Containment after Loss of Coolant Accident, In: International Symposium on Mechanics of Composites, ed. M. Černý, CTU in Prague, Klokner Institute, Prague 2002, p. 91
[13] Králik J., Cesnak J.: Nonlinear Analysis of Power Plant Buildings with the VVER 230 Reactor After a Loss off Coolant Accident, Slovak Journal of Civil Engineering 8 (2000) 18
[14] Králik J.: Probability Nonlinear Analysis of Reinforced Concrete Containment Damage due to High Internal Overpressure, Engineering Mechanics 12 (2005) 113
[15] Králik J.: Comparison of Probabilistic Methods Efficiency to Solve the Structure Reliability in FEM, In: IX. Int. Conf. on Reliability of Structures, Prague 2008, p. 41
[16] Králik J.: Reliability Analysis of Structures Using Stochastic Finite Element Method, Habilitation work, Edition STU Bratislava 2009, Bratislava
[17] Králik J.: Safety and Reliability of Nuclear Power Buildings in Slovakia. Earthquake-Impact-Explosion, Edition STU Bratislava 2009, Bratislava
[18] Kupfer H., Hilsdorf H.K., Ruesch H.: Behavior of Concrete Under Biaxial Stresses, Journal ACI 66 (1969) 656
[19] Lenkei P., Györgyi J.: Probabilistic Structural Analysis of Nuclear Containment under LB LOCA. Report JE Paks, N-Quad Ltd. 1999, Pécs
[20] Li C.Q.: Time Dependent Reliability Analysis of the Serviceability of Corrosion Affected Concrete Structures, International Journal of Materials & Structural Reliability 3 (2005) 105
[21] Meskouris K., Wittek U.: Aspects in Modern Computational Structural Analysis, A.A. Balkema Publishers 1997, Rotterdam
[22] Oñate E., Oller S., Oliver J., Lubliner J.: A Constitutive Model for Cracking of Concrete Based on the Incremental Theory of Plasticity, Engineering Computation 5 (1993) 309
[23] Rosowsky D.V.: Structural Reliability. Part of 'Structural Engineering Handbook', ed. Chen Wai-Fah, Boca Raton, CRC Press LLC 1999
[24] Řeřicha P., Šejnoha J.: Partial Service Life Assessment of a Reactor Containment, Nuclear Engineering Design 235 (2008) 2451
[25] Teplý B., Chromá M., Rovnaník P.: Durability Assessment of Concrete Structures: Reinforcement Depassivation due to Carbonation, Structure and Infrastructure Engineering, 6 (2010) 317
[26] Vejvoda S., Keršner Z., Novák D., Teplý B.: Probabilistic Safety Assessment of the Steam Generator Cover, In: SMiRT17, 17th International Conference on Structural Mechanics in Reactor Technology, Prague 2003, CD-ROM
[27] Žmindák M., Novák P., Nozdrovický J., Melicher R.: Thermomechanic Analysis of Reinforced Reactor Shaft Structure, Acta Mechanica Slovaca, 3 (2008) 133 (in Slovak)

Received in editor's office: June 11, 2009
Approved for publishing: August 19, 2010